Interaction of presenilins with FKBP38 promotes apoptosis by reducing mitochondrial Bcl-2

Hua-Qin Wang[1,2,†], Yoshifumi Nakaya[1,†], Zhenyu Du[1], Takuya Yamane[1], Michiko Shirane[3], Takashi Kudo[4], Masatoshi Takeda[4], Koichi Takebayashi[2], Yoichi Noda[2], Keiichi I. Nakayama[3] and Masaki Nishimura[1,*]

[1]Neurology Unit, Molecular Neuroscience Research Center, and [2]Department of Obstetrics and Gynecology, Shiga University of Medical Science, Otsu, Shiga 520-2192, Japan

[3]Department of Molecular and Cellular Biology, Medical Institute of Bioregulation, Kyushu University, Fukuoka, Fukuoka 812-8582, Japan

[4]Department of Post-Genomics and Diseases, Division of Psychiatry and Behavioral Proteomics, Osaka University Graduate School of Medicine, Suita, Osaka 565-0871, Japan

[*]To whom correspondence should be addressed at: Molecular Neuroscience Research Center, Shiga University of Medical Science, Seta-Tsukinowacho, Otsu, Shiga 520-2192, Japan

Tel: +81 77 548 2327; Fax: +81 77 548 2402; E-mail: mnishimu@belle.shiga-med.ac.jp

[†]Present address: Department of Neurology, Kyoto University Graduate School of Medicine, Kyoto, Kyoto 606-8507, Japan

Presenilins 1 and 2 (PS1/2), causative molecules for familial Alzheimer's disease (FAD), are multipass transmembrane proteins localized predominantly in the endoplasmic reticulum (ER) and Golgi apparatus. Heteromeric protein complexes containing PS1/2 are thought to participate in several functions, including intramembrane proteolysis mediated by their γ-secretase activities. Previous studies have shown that PS1/2 are also involved in the regulation of apoptotic cell death, although the underlying mechanism remains unknown. Here, we demonstrate that FKBP38, an immunophilin family member residing in the mitochondrial membrane, is an authentic PS1/2-interacting protein. PS1/2 and FKBP38 form macromolecular complexes together with anti-apoptotic Bcl-2. PS1/2 promote the degradation of FKBP38 and Bcl-2, and sequester these proteins in the ER/Golgi compartments, thereby inhibiting FKBP38-mediated mitochondrial targeting of Bcl-2 *via* a γ-secretase-independent mechanism. Thus, PS1/2 increase the susceptibility to apoptosis by antagonizing the anti-apoptotic function of FKBP38. In contrast, C-terminal fragments of caspase-processed PS1/2 redistribute Bcl-2 to the mitochondria by abrogating the activity of full-length PS1/2, resulting in a dominant-negative anti-apoptotic effect. In cultured cells and mutant PS1-knockin mouse brains, FAD-linked PS1/2 mutants enhance the pro-apoptotic activity by causing a more efficient reduction in mitochondrial Bcl-2 than wild-type PS1/2. These results suggest a novel molecular mechanism for the regulation of mitochondria-mediated apoptosis by competition between PS1/2 and FKBP38 for subcellular targeting of Bcl-2. Excessive pro-apoptotic activity of PS1/2 may play a role in the pathogenesis of FAD.

INTRODUCTION

Apoptotic cell death is an essential process required for development and maintenance of normal tissues, but it is also involved in various pathological conditions. Mitochondria play a pivotal role in the intrinsic pathway of apoptosis, wherein various apoptotic stimuli converge to cause increased permeability of the outer mitochondrial membrane, resulting in the release of mitochondrial apoptogenic proteins, such as cytochrome *c* and Smac/Diablo, into the cytosol (1). Mitochondrial membrane permeability is negatively and positively regulated by anti-apoptotic and pro-apoptotic members of the Bcl-2 family, respectively (2, 3). The ratio of anti- to pro-apoptotic members and the mitochondrial localization critically influence the susceptibility to apoptosis (2-4).

Alzheimer's disease (AD), the most common cause of dementia in the elderly, is neuropathologically characterized by prominent neuronal loss with astrogliosis and by the appearance of extracellular amyloid plaques and intracellular neurofibrillary tangles in the cerebral cortex. Excessive accumulation of amyloid β (Aβ) peptide, which is the major constituent of amyloid plaques, is thought to trigger a pathological cascade leading to neurodegeneration in AD. However, the chronic progression of the degeneration in AD has made it difficult to elucidate the mechanism of neuronal loss. Although the contribution of apoptosis to neuronal death in AD brains is still controversial, a number of previous reports have demonstrated the potential involvement of Aβ peptide and its precursor protein in the induction or regulation of apoptotic neuronal death (reviewed in 5-7). In addition, circumstantial evidence of apoptosis in postmortem brain tissues has supported the hypothesis that an apoptotic mechanism plays a role in the neurodegeneration in AD (8, 9).

Mutations in presenilins 1 and 2 (PS1/2) are responsible for the majority of autosomal dominant forms of familial Alzheimer's disease (FAD) (10). These two proteins are highly homologous and consist of eight transmembrane domains and a large hydrophilic loop between transmembrane domains 6 and 7. Presenilins are ubiquitously expressed, and undergo physiological endoproteolytic cleavage, yielding N- and C-terminal fragments (NTF and CTF, respectively). The accumulation of these proteolytic derivatives *in vivo* is tightly regulated and saturable (11), suggesting that constitutive levels of expression are crucial for cell function.

Independent of the original cloning of PS1/2 as genes causing FAD, functional screening

identified a truncated mouse homologue of PS2 (referred to as ALG-3) as an apoptosis-linked molecule (12). Overexpression of PS2 in diverse cell types leads to enhanced susceptibility to various apoptotic stimuli, whereas suppression of PS2 expression by antisense RNA reduces the apoptotic susceptibility of PC12 cells (13, 14). Moreover, FAD-linked mutations of both PS1 and PS2 potentiate their pro-apoptotic properties in cultured cells and in neurons from mutant PS1-knockin mice (13, 15-23). Meanwhile, PS1/2 are cleaved by activated caspase-3 family proteases during apoptosis in cultured cells (24). Similar to the ALG-3 polypeptide, overexpression of polypeptides corresponding to the C-terminal PS1/2 fragments generated by caspase cleavage inhibits apoptosis (25, 26). These findings strongly suggest that PS1/2 are involved in the regulation of apoptosis under physiological and pathological conditions. However, the molecular mechanism underlying these observations remains to be elucidated.

In addition to regulation of apoptosis, PS1/2 have been implicated as unique aspartyl proteases, referred to as γ-secretase, that mediate the intramembrane cleavage of various type-I transmembrane proteins (27), scaffolding proteins that facilitate the phosphorylation of β-catenin (28), and modulators of cellular calcium homeostasis (29). PS1/2 proteins become stabilized and functional after assembly into each heteromeric macromolecular complex. The essential components of PS complexes include at least three membrane proteins, nicastrin, APH-1 and PEN-2. These complexes participate in a variety of functions, probably by interacting with multiple sets of effector proteins.

Here, we identified FK506-binding protein 38 (FKBP38) as a novel PS-binding partner. Among FKBP family members, FKBP38 is unique in displaying neither an affinity for FK506 nor peptidyl-prolyl *cis/trans*-isomerase activity (30-32). High-molecular weight immunophilins, including FKBP38, FKBP51, FKBP52, and CyP40, are structurally characterized by tetratricopeptide repeats (TPRs) that mediate protein-protein interaction (30, 31, 33). Additionally, FKBP38 has a transmembrane domain at its C-terminus and is predominantly localized in the mitochondrial membrane (33). A recent study revealed that FKBP38 inhibits apoptosis by targeting and anchoring anti-apoptotic Bcl-2 to the mitochondria (33). Here, we demonstrate that the pro-apoptotic function of PS1/2 is due to competition with the anti-apoptotic activity of FKBP38. Caspase-processed C-terminal fragments of PS1/2 abrogate the antagonizing action of full-length (FL) PS1/2 on FKBP38, exhibiting

a dominant-negative anti-apoptotic effect, whereas FAD-linked mutations of PS1/2 cause enhanced inhibition of FKBP38 activity.

RESULTS

PS1/2 specifically interact with FKBP38

To clarify the molecular basis by which PS1/2 regulate apoptosis, we first searched for proteins that interact with the PS1 CTF, a highly conserved region that is likely responsible for the modulation of apoptosis (25). We performed a yeast two-hybrid screen of a HeLa cell cDNA library using the human PS1 C-terminal sequence (residues 351-467) as bait. We isolated seven positive clones by screening 3.5×10^6 transformants and confirmed the interaction by a yeast mating assay on a high stringency medium. DNA sequencing and BLAST searches revealed that two of these clones encoded full-length FKBP38.

Binding between PS1/2 and FKBP38 in mammalian cells was then examined. Human FKBP38 fused at its C-terminus to a Myc epitope tag (FKBP38-Myc) was transiently transfected into human embryonic kidney 293 (HEK293) cells along with PS1 or PS2. We found that PS1 and PS2 coimmunoprecipitated with FKBP38-Myc but not with other TPR-containing immunophilins, including CyP40-Myc, FKBP51-Myc, and FKBP52-Myc (Fig. 1A). Although PS1 and PS2 were expressed at similar levels, in all experiments, larger amounts of PS2 coprecipitated with FKBP38-Myc when compared with PS1. In addition, endogenous PS1 and PS2 coprecipitated with FKBP38 in HEK293 cell lysates (data not shown).

To confirm a physiological interaction between PS1/2 and FKBP38, we examined their endogenous binding in lysates of murine brains. We found that FKBP38 coprecipitated with both PS1 and PS2 (Fig. 1B). The specificity of this interaction was supported by the lack of binding to calnexin, an endoplasmic reticulum (ER)-associated protein, as well as by confirmation of binding by Bcl-2, a known FKBP38-binding protein (33). Similar to the HEK293 experiments, a larger amount of FKBP38 coprecipitated with PS2 than with PS1.

We next assessed the binding of PS1/2 to a dominant-negative mutant, FKBP38$^{\Delta TM}$, that lacks the transmembrane domain and the ability to localize in the mitochondria (33). We found that similar amounts of haemagglutinin A-tagged FKBP38$^{\Delta TM}$ (FKBP38$^{\Delta TM}$-HA) and full-length

FKBP38-HA were detected in immunoprecipitates with an anti-PS1 CTF or anti-PS2 CTF antibody (Fig. 1C). Together with the results of the two-hybrid screen, this indicates that PS1/2 CTFs interact with the N-terminal region of FKBP38, which contains TPR domains (30, 31).

Both PS1 and FKBP38 have been reported to associate with Bcl-2 (33, 34). To investigate the binding mode between these three proteins, we performed coimmunoprecipitation assays with PS1/2- and/or FKBP38-depleted cell lysates. As described previously (33), RNA interference (RNAi) using a small interfering RNA (siRNA) duplex successfully reduced the endogenous expression of FKBP38 in mouse embryonic fibroblasts (MEFs). In agreement with prior reports (33, 34), anti-Bcl-2 antibody coprecipitated PS1, PS2, and FKBP38 in native cell lysates (Fig. 1D). Whereas FKBP38 coprecipitated with Bcl-2 in lysates from PS1- and PS2-double knockout (PS1/2-null) cells, only trace levels of PS1 and PS2 coimmunoprecipitated with Bcl-2 in lysates from FKBP38 knockdown cells (Fig. 1D). This result suggests that association of PS1/2 with Bcl-2 is largely mediated through their binding to FKBP38.

PS1/2, FKBP38, and Bcl-2 are components of multiprotein complexes

Based on the ability of PS1/2 to associate with FKBP38 and Bcl-2, we suspected that these proteins are components of heteromeric complexes. We investigated this possibility using glycerol velocity gradient centrifugation analysis of native HEK293 cell extracts (Fig. 2A). As previously reported (35), NTF and CTF of endogenous PS1 formed complexes of ~200 to 400 kDa. FKBP38 was detected in a molecular weight range above 200 kDa, which is substantially higher than that of the 38 kDa monomer. Bcl-2 is distributed in a range between 60 and 300 kDa. FKBP38 and Bcl-2 partially overlapped with PS1 in fractions 6 to 8, suggesting that restricted subsets of these proteins bind with PS1 (Fig. 2A). Because PS2 is expressed at a low level in native cells, we used HEK293 cells stably transfected with PS2 to examine its complex formation. In this system, the relative molecular weight of PS2 CTF-containing complex was similar to that of the PS1 complex, whereas uncleaved PS2 holoprotein was distributed over the lower molecular weight range (Fig. 2A). To further confirm the binding between these proteins, we performed coimmunoprecipitation of fractionated samples. We found that both FKBP38 and Bcl-2 coprecipitated with PS1 or PS2 in fractions 6 to 8 (Fig. 2B and data not shown), supporting the notion that PS1/2 form complexes with FKBP38 and Bcl-2.

Deletion of PS1/2 reduces susceptibility to mitochondria-mediated apoptosis

A recent study has revealed that FKBP38 is an anti-apoptotic protein (33). Therefore, it is possible that the interaction between PS1/2 and FKBP38 is related to the regulation of apoptosis. We first estimated the susceptibility to apoptosis of MEFs from PS1- and/or PS2-knockout mice. After treatment with apoptotic agents, cell viability and apoptosis were quantified by 3-(4,5-dimethylthiazal-2-yl)-2,5-diphenyltetrazolium bromide (MTT) conversion and annexin V/propidium iodide (PI) staining, respectively. PS1-null, PS2-null, and PS1/2-null MEFs were significantly less sensitive than native MEFs to induction of apoptotic cell death by staurosporine or A23187 (Fig. 3A and B). The effect of PS2 deletion was more potent than that of PS1 deletion ($p < 0.001$ by one-way ANOVA with Dunnett's *post-hoc* test), and the effects of PS1 and PS2 deletion were additive. A similar result was obtained when these MEFs were treated with rapamycin (0.1 μg/ml) or etoposide (20 μM) (data not shown). In subsequent experiments, we used PS1/2-null MEFs to avoid compensation for the loss of either of the two proteins.

We further examined the contribution of PS1/2 to apoptosis by assessing its effects on mitochondria-mediated apoptosis signaling, which involves cytochrome *c* release from the mitochondria to the cytosol. As shown in Fig. 3C, under basal conditions (vehicle control), cytochrome *c* was not detected in the cytosol fraction from either native or PS1/2-null MEFs. A 24-h treatment with staurosporine or A23187 induced translocation of cytochrome *c* from the membrane to the cytosol in native MEFs. This translocation was less prominent in PS1/2-null MEFs, suggesting that PS1/2 deletion results in decreased sensitivity to mitochondria-mediated apoptosis.

PS1/2 promote the degradation of FKBP38 and Bcl-2

PS1/2 are required for the proper expression of certain PS-binding proteins. For example, PS1/2 deletion downregulates the accumulation of PEN-2 and the maturation of nicastrin (27). In contrast, immunoblotting unexpectedly showed that the relative band intensities for FKBP38 and Bcl-2 in PS1/2-null MEFs increased by ~81% and ~58%, respectively, when compared with native MEFs (mean of three independent blots; $p < 0.01$ by Student's-*t* test; Fig. 4A). Semi-quantitative RT-PCR revealed that native and PS1/2-null MEFs expressed similar levels of FKBP38 and Bcl-2 mRNA (Fig. 4B). However, as shown in Fig. 4C, the half-life of FKBP38 protein in the presence of

cycloheximide was significantly longer in PS1/2-null than in native MEFs (mean ± SD; 17.2 ± 0.9 h *vs*. 10.5 ± 0.7 h [n = 4], respectively; $p < 0.01$ by Student's-*t* test). A similar increase in the half-life of Bcl-2 protein in PS1/2-null MEFs was observed (mean ± SD; 35.7 ± 1.9 h *vs*. 23.4 ± 1.3 h [n = 4], respectively; $p < 0.01$ by Student's-*t* test). Transfection of PS1 or PS2 into PS1/2-null MEFs decreased the half-lives of these proteins (data not shown). Finally, pulse-chase experiments confirmed that the rate of FKBP38 translation was equivalent in native and PS1/2-null MEFs but that there was a clear delay in FKBP38 degradation in PS1/2-null MEFs (Fig. 4D). A similar result was obtained for Bcl-2 (data not shown). Taken together, these results suggest that PS1/2 destabilize FKBP38 and Bcl-2 proteins, decreasing their steady-state levels without affecting the rates of transcription or translation.

FKBP38 is not a substrate for the γ-secretase activity of PS1/2 complexes

PS1/2 are catalytic components of γ-secretase complexes that mediate intramembrane cleavage of amyloid β-precursor protein (APP) and several other type I membrane proteins (27). We therefore tested the possibility that PS1/2 degrade FKBP38 through their γ-secretase activities. We first checked for the release of cleavage products from the membrane, but we were unable to detect any discernible bands in the cytosol and cell culture medium by immunoblotting (Fig. 5A). Treatment of cells with the potent γ-secretase inhibitors DFK167, DAPT, or L-685,458 (36) caused accumulation of APP CTF, which is a direct substrate for γ-secretase. However, these inhibitors did not affect the accumulation level of FKBP38 (Fig. 5B). To detect size reduction by intramembrane cleavage, we generated a FKBP38 construct fused to the N-terminus of green fluorescent protein (GFP). Anti-GFP immunoblotting of HEK293 cells transfected with this fusion protein and treated with or without DFK167 revealed only a 60-kDa band representing the intact fusion protein (Fig. 5C). Together with the prediction that FKBP38 is a type II membrane protein (33), these results suggest that FKBP38 is not a substrate for γ-secretase.

PS1/2 sequester FKBP38 and Bcl-2 in the ER/Golgi compartments

The anti-apoptotic function of FKBP38 is mediated by targeting and anchoring Bcl-2 to mitochondria (33). We investigated whether PS1/2 alter the subcellular localization of FKBP38 and Bcl-2. Under physiological conditions, the majority of FKBP38 and Bcl-2 is localized in the

mitochondria, while a smaller amount is found in the ER/Golgi and nuclear envelope (33, 37). In contrast, PS1/2 is predominantly distributed in the ER/Golgi and, to a lesser extent, in the plasma membrane, nuclear envelope, and mitochondria (38-40). Double fluorescence staining revealed that the mitochondrial localization of FKBP38 was more prominent in PS1/2-null than in native MEFs (Fig. 6A, yellow signals in the merged images). A similar increase in the mitochondrial Bcl-2 was observed in PS1/2-null MEFs (Fig. 6B).

To confirm this result, we employed subcellular fractionation of vesicular organelles on an iodixanol gradient, which considerably separated the mitochondria (fractions 1 to 5) from the ER/Golgi (fractions 5 to 10) (Fig. 6C). As expected, in native MEFs, PS1 CTF were identified in the ER/Golgi fractions, whereas FKBP38 was recovered from both the mitochondrial and ER/Golgi fractions. In contrast, in PS1/2-null MEFs, FKPB38 was detected only in mitochondria-rich fractions. Similarly, in the native cells, there were two broad Bcl-2 peaks, corresponding to the mitochondrial and ER/Golgi fractions, whereas in PS1/2-null MEFs, the ER/Golgi peak disappeared and the mitochondrial peak increased (Fig.6C). Together with immunocytochemical studies, these observations imply that, under normal conditions, PS1/2 sequester FKBP38 and Bcl-2 in the ER/Golgi compartments, reducing their levels in mitochondria. Consistent with the result that PS1/2 do not bind to CyP40, FKBP51 or FKBP52 (Fig. 1A), Hsp90 heteromeric complexes, which contain these immunophilins (41), were not associated with membranous organelles in the absence or presence of PS1/2 (data not shown).

In addition, we investigated the effect of FKBP38 depletion on the subcellular localization of Bcl-2. When FKBP38 was depleted in native MEFs by RNAi, Bcl-2 was markedly diminished in the mitochondrial fractions and was predominantly distributed in the ER/Golgi fractions (Fig. 6D, left panel). As predicted by our coimmunoprecipitation results, which suggested that PS1/2 associate with Bcl-2 *via* FKBP38 (Fig. 1D), FKBP38 knockdown by RNAi abrogated the effect of PS1/2 on the subcellular distribution of Bcl-2. Thus, FKBP38 depletion in PS1/2-null MEFs resulted in a similar pattern of Bcl-2 distribution as that found in FKBP38-depleted native MEFs (Fig. 6D).

Promotion of apoptosis by PS1/2 corresponds with a reduction in mitochondrial Bcl-2

We reasoned that the pro-apoptotic activity of PS1/2 might be mediated through their

binding to FKBP38 and the subsequent reduction of mitochondrial Bcl-2. PS1/2 deletion decreased the apoptotic susceptibility, whereas overexpression of wild-type (WT) PS2 significantly sensitized cells to staurosporine-induced apoptosis when compared with native cells (Fig. 7A, compare PS1/2-null or WT PS2-overexpressing with native MEFs). The total amount of FKBP38 or Bcl-2 inversely correlated with the level of PS1/2 (Fig. 7B and see also 42 and 43). Furthermore, subcellular fractionation revealed that PS1/2 deletion increased Bcl-2 in the mitochondrial fractions (Fig. 6C), whereas PS2 overexpression reduced mitochondrial Bcl-2 by sequestering it in the ER/Golgi (Fig. 7C, compare WT PS2-overexpressing with native MEFs). Exogenous overexpression of FKBP38 could reduce the pro-apoptotic effect of co-overexpressed PS2 by redistributing Bcl-2 from the ER/Golgi to the mitochondria (Figs. 7A and C, compare WT PS2 + FKBP38-overexpressing with WT PS2-overexpressing MEFs). In contrast, expression of C-terminally truncated PS2 (residues 1-350), which does not bind with FKBP38, neither enhanced the apoptotic susceptibility nor altered the localization of Bcl-2 in native or PS1/2-null MEFs (data not shown). Furthermore, when overexpressing a dominant-negative mutant FKBP38$^{\Delta TM}$, which markedly increased the apoptotic susceptibility by shifting Bcl-2 to the cytosol (33), or when FKBP38 was depleted by RNAi, native and PS1/2-null MEFs exhibited a similar apoptosis susceptibility and Bcl-2 localization (Fig. 6D, and data not shown). These results indicate that the promotion of apoptosis by PS2 is mediated by its binding to FKBP38 and corresponds with a reduction in mitochondrial Bcl-2. PS1/2 appear to compete with FKBP38 for subcellular targeting of Bcl-2.

We next examined the anti-apoptotic activity of a polypeptide corresponding to caspase-3-processed PS2 CTF (PS2 CTF^{CAS}; corresponding to residues 329-448 of PS2 along with an initiating methionine) (25, 26). Upon iodixanol fractionation, exogenous PS2 CTF^{CAS} was more broadly distributed than the physiologically processed PS2 CTF (Fig. 7D). Overexpression of PS2 CTF^{CAS} in native MEFs significantly decreased the sensitivity to staurosporine-induced apoptosis and shifted Bcl-2 from the ER/Golgi to the mitochondrial fractions (Figs. 7A and C, compare PS2 CTF^{CAS}-overexpressing with native MEFs). PS2 CTF^{CAS}-overexpressing MEFs had a similar viability and Bcl-2 localization as PS1/2-null MEFs, suggesting that PS2 CTF^{CAS} abrogated the pro-apoptotic activity of endogenous PS1/2 by impeding sequestration of Bcl-2 in the ER/Golgi. Overexpression of

PS2 CTF^{CAS} also caused a reduction in endogenous PS1/2 coimmunoprecipitating with FKBP38 (data not shown). These results suggest that exogenous PS2 CTF^{CAS}, which contains the FKBP38 binding domain but presumably lacks the ability to sequester FKBP38 and Bcl-2 in the ER/Golgi, compete with endogenous PS1/2 for binding to FKBP38, thus resulting in a dominant-negative effect. Consistent with a previous report (25), similar results were obtained with polypeptides corresponding to the physiological CTF of PS2 (residues 298-448) (data not shown).

FAD-linked mutations of PS1/2 enhance the sequestration of Bcl-2 in the ER/Golgi

We further investigated the pro-apoptotic effects of FAD-linked mutants (N141I- and M239V-PS2). In agreement with prior reports (15, 16, 43), the apoptosis susceptibility of PS1/2-null MEFs was more enhanced when they overexpressed FAD-linked PS2 than when they overexpressed WT PS2 (Fig. 7A, compare N141I- or M239V-PS2-overexpressing with WT PS2-overexpressing MEFs). In addition, N141I-PS2 sequesters more Bcl-2 in the ER/Golgi fractions than WT PS2 (Fig. 7C, compare N141I-PS2-overexpressing with WT PS2-overexpressing MEFs), although the expression levels and subcellular distribution of N141I- and WT PS2 were equivalent (Fig. 7D). Similar results were obtained with FAD-linked (I143F and L392V) PS1 (data not shown).

To exclude the possibility that this mutational effect was caused by overexpression of mutant PS, we performed iodixanol fractionation of brain homogenates from FAD-linked mutant (I213T) PS1-knockin mice (44). Primary cultured neurons from FAD-linked mutant PS1-knockin mice have been reported to exhibit the enhanced susceptibility to apoptosis induced by various stimuli (20, 45). As shown in Fig. 7E, I213T mutation obviously shifted Bcl-2 distribution from the mitochondria to the ER/Golgi fractions in a gene dosage-dependent manner. This suggests that a physiological level of FAD-linked mutant PS1 can modify the subcellular distribution of Bcl-2.

The pro-apoptotic function of PS2 is independent of γ-secretase activity

Finally, to assess the relationship between the pro-apoptotic function of PS1/2 and γ-secretase activity, we treated native MEFs with DFK167, DAPT, or L-685,458. We found that these γ-secretase inhibitors had no effect on the localization of Bcl-2 (data not shown). We also examined the effects of D366A-PS2, which has no γ-secretase activity, in PS1/2-null MEFs. Subcellular distribution of transfected D366A-PS2 was similar to that of WT PS2 FL (Fig. 7D). When compared

with WT PS2-transfected MEFs, there were no differences in apoptotic susceptibility or subcellular localization of Bcl-2 (Figs. 7A and C, compare D366A-PS2-overexpresing with WT PS2-overexpressing MEFs), suggesting that the pro-apoptotic function of PS2 is independent of γ-secretase activity.

DISCUSSION

Using a yeast two-hybrid screen and other supportive methods, we identified FKBP38 as a directly interacting partner of PS1/2 proteins. Comparative studies using native and PS1/2-null cells disclosed the consequences of this interaction, although a relatively small pool of FKBP38 appeared to bind with PS1/2. We showed that the ablation of PS1/2 led to a slower turnover of FKBP38 protein and a more restricted localization of FKBP38 in the mitochondria. Thus, PS1/2 facilitate the degradation of FKBP38 in a γ-secretase-independent fashion, and sequester FKBP38 in the ER/Golgi compartments, thereby reducing the amount of mitochondrial FKBP38.

Previous reports have shown an interaction between PS1 and Bcl-2 as well as between FKBP38 and Bcl-2 (33, 34). We observed that these membrane proteins are incorporated into macromolecular complexes. Bcl-2 coimmunoprecipitated with FKBP38 even in the absence of PS1/2, but that a very small amount of Bcl-2 coprecipitated with PS1 or PS2 in FKBP38-depleted cell lysates. This result suggests that PS1/2 are associated with Bcl-2 mainly by binding with FKBP38, although our result does not completely eliminate the possibility that PS1/2 have a weak binding affinity to Bcl-2. This is concordant with the previous report showing that Bcl-2 coimmunoprecipitated with PS1 in Bcl-2-overexpressing but not in native H4 neuroglioma cells (34). PS1/2 downregulate the accumulation level of Bcl-2, and sequester Bcl-2 in the ER/Golgi compartments in an expression level-dependent manner. As a result, the amount of mitochondrial Bcl-2 increases in the absence of PS1/2 and decreases when overexpressing PS1/2.

Our results indicate that PS1/2 modulate the susceptibility to apoptosis by regulating the subcellular localization of Bcl-2 *via* binding to FKBP38. The representative anti-apoptotic members of the Bcl-2 family, Bcl-2 and Bcl-X_L, primarily function on the outer mitochondrial membrane (reviewed in 2-4). Bcl-X_L has a targeting signal for the mitochondria, but Bcl-2 does not (46). Recent studies have suggested that binding to anchor proteins residing in specific compartments is an

important determinant of the subcellular distribution of Bcl-2 and Bcl-X_L. Thus, FKBP38 is responsible for the mitochondrial localization of Bcl-2 and Bcl-X_L (33), whereas overexpression of reticulon family members (*i.e.*, RTN-X_S and NSP-C) sensitizes cells to apoptosis by increasing the localization of Bcl-X_L on the ER (47). Exogenously expressed RTN-X_S also induces the localization of Bcl-2 on the ER to a lesser extent (47). Our results indicate that PS1/2 shift Bcl-2 from the mitochondria to the ER/Golgi in an expression level-dependent manner. The pro-apoptotic activity of PS1/2 correlates well with the reduction in mitochondrial Bcl-2, and this can be antagonized by overexpression of FKBP38. Thus, PS1/2 compete with FKBP38 for regulation of the amount of mitochondrial Bcl-2, and this competition probably depends on the relative levels of FKBP38 and PS1/2. The more potent effect of PS2 (relative to PS1) may be due to its higher affinity for FKBP38 (see Figs. 1A, 1B, 3A and 3B). PS1/2 have been reported to bind to Bcl-X_L as well as Bcl-2 (48), but we could not detect obvious effects of PS1/2 on the subcellular localization of Bcl-X_L (data not shown). These results indicate that PS1/2 and reticulon family members are predominantly responsible for the ER/Golgi localization of Bcl-2 and Bcl-X_L, respectively.

PS1/2 are substrates for effector caspases that execute the apoptotic death process. Thus, PS1/2 undergo alternative endoproteolysis during apoptosis, which can be blocked by zDEVD-fmk, an inhibitor of caspase-3 family proteases (24, 25). This cleavage yields C-terminal polypeptides, PS1/2 $CTFs^{CAS}$, which are shorter than physiologically processed CTFs (PS1/2 $CTFs^{PHY}$). Our results indicate that PS1/2 $CTFs^{CAS}$ competes with FL PS1/2 for binding to FKBP38 and thereby acts as a dominant-negative inhibitor of Bcl-2 sequestration in the ER/Golgi. Thus, the generation of PS1/2 $CTFs^{CAS}$ by activated caspases may constitute a negative feedback loop in apoptosis signaling. Similar to PS2 CTF^{CAS}, PS2 CTF^{PHY} exhibited anti-apoptotic activity (25). However, PS1/2 $CTFs^{PHY}$ are incorporated into PS complexes together with PS1/2 NTFs immediately after the physiological cleavage, and the monomeric PS1/2 $CTFs^{PHY}$ cannot be detected in normal cells (35). Therefore, PS1/2 $CTFs^{PHY}$ are unlikely to contribute to the anti-apoptotic activity.

Several apoptosis signaling events have been implicated in PS-induced apoptosis, which include activation of p53 (23, 49) or p38 mitogen activated protein kinases (50), downregulation of Akt/protein kinase B signaling (51) or unfolded protein response signaling (52), destabilization of

β-catenin (53), and perturbed calcium homeostasis (17, 54). PS1/2 might be directly or indirectly involved in multiple pathways for cell death. However, we have concluded that the pro-apoptotic activity of PS1/2 mainly dependents on their binding with FKBP38 and a reduction of mitochondrial Bcl-2 for the following reasons. First, overexpression of FKBP38 could neutralize the pro-apoptotic activity of PS1/2 by redistributing Bcl-2 from the ER/Golgi to the mitochondria. Second, in FKBP38-deleted cells, PS1/2 did not have the pro-apoptotic activity and effect on localization of Bcl-2. Third, PS2 CTF^{CAS} decreased the sensitivity to apoptosis and simultaneously shifted Bcl-2 from the ER/Golgi to the mitochondria in a dominant-negative manner. Fourth, C-terminally truncated PS2 that lacks the binding site for FKBP38 had no effect on apoptosis susceptibility and Bcl-2 localization. We thought that the inactivity of this truncated PS2 was not only due to instability of this polypeptide, because transfected PS2 CTF had the anti-apoptotic activity in spite of the similar instability (55).

PS complexes are involved in many vital functions through binding to various proteins in addition to forming the γ-secretase complexes together with three essential components. The absence of PS1/2 results in the downregulation of the essential component proteins (27), although PS1/2 binding does not lead to alteration in the accumulation levels of many other interacting proteins. By contrast, we found that PS1/2 destabilize FKBP38 and Bcl-2. Similar to this observation, previous studies have shown that PS1/2 promote the degradation of β-catenin by facilitating its phosphorylation (28), and that, in hippocampal neurons, PS1/2 increase the turnover of the neuron-specific cell adhesion molecule telencephalin by enhancing autophagic vacuole-mediated catabolism (56, 57). Our results and these findings indicate a γ-secretase-independent function for PS1/2 in regulating the accumulation level of effector proteins.

The molecular pathomechanism by which PS1/2 mutations cause AD is not entirely clear, although FAD-linked mutations are known to enhance the production of long, pathogenic Aβ peptides through altering γ-secretase cleavage by PS complexes (reviewed in 58). Oligomerized forms of Aβ have been implicated in the pathogenesis in AD due to both deleterious effects on synaptic plasticity and toxic effects that induce neuronal death (59, 60). In addition to neurotoxicity of Aβ, several other pathological conditions such as oxidative stress, impaired calcium homeostasis, and mitochondrial dysfunction are observed in AD brains (reviewed in 61). These apoptosis-inducing stimuli may

accelerate the irreversible and pathological processes in AD brains, and mitochondria can act not only as mediators but also as amplifiers of apoptosis signaling. Our results suggest that FAD-linked mutations in PS1/2 lower the threshold for activation of mitochondria-mediated apoptosis pathways in neurons of individuals with FAD. In cases of sporadic AD, for which the primary causes are still unclear, yet unidentified factors besides PS mutations could contribute to disease progression by enhancing the pro-apoptotic activity of PS1/2. Therefore, blockers of endogenous binding between PS1/2 and FKBP38, such as polypeptides spanning the PS1/2 CTF sequences, might be beneficial in the treatment of AD by preventing the enhancement of apoptosis by PS1/2.

MATERIAL AND METHODS

Yeast two-hybrid screen

The bait vector pGBKT7-PS1C, encoding the C-terminal sequence of PS1 fused to the GAL4 DNA binding domain, was generated by subcloning the PCR-amplified PS1 fragment into pGBKT7, which is free of autonomous β-galactosidase activity. Yeast two-hybrid screening was performed on a human HeLa cell cDNA library according to the manufacturer's instructions (Clontech, San Diego, CA, USA). Briefly, yeast strain AH109 was cotransformed with pGBKT7-PS1C and pACT2 containing library cDNAs fused to the GAL4 transcription activation domain. The transformants were selected on plates lacking histidine, tryptophan, lysine, and leucine. Positive clones were identified after seven days, and yeast mating assays were performed to confirm the interaction in yeast. Candidate cDNAs for PS1-interacting proteins were isolated, sequenced, and analyzed using the BLASTN program.

cDNA constructs, antibodies, and reagents

Eukaryotic expression vectors for PS1 and PS2 were previously described (62). Constructs for various truncation mutants for PS1 and PS2 were prepared by subcloning the PCR-amplified fragments into pcDNA3.1 (Invitrogen, Carlsbad, CA, USA). Expression vectors for FKBP38-Myc, FKBP51-Myc, FKBP52-Myc and CyP40-Myc were generated by subcloning the sequence-verified RT-PCR products into pcDNA4/Myc-His (Invitrogen). FKBP38 fused to GFP was subcloned into pEGFP-N1 (Clonetech). The FKBP38-HA and FKBP38$^{\Delta TM}$-HA constructs and the rabbit polyclonal antibody against the N-terminus of FKBP38 were prepared as described (33). Monoclonal antibodies

were purchased for PS1 CTF (Chemicon, Temecula, CA, USA), cytochrome *c* (BD Pharmingen, San Diego, CA, USA), adaptin-γ (Transduction Laboratories, Lexington, KY, USA), cyclooxygenase-IV (Molecular Probes, Eugene, OR, USA), HA (Roche Diagnostics, Mannheim, Germany), and GFP (Nacalai, Kyoto, Japan). The polyclonal antibodies were obtained for PS1 NTF (Zymed, South San Francisco, CA, USA), PS2 CTF (Cell Signaling, Beverly, CA, USA), APP (Sigma, St. Louis, MO, USA), and calnexin (Stressgen, San Diego, CA, USA). Polyclonal anti-PS2 NTF, anti-Hsp90, monoclonal anti-Myc tag (9E10), and anti-Bcl-2 antibodies were from Santa Cruz Biotechnology (Santa Cruz, CA, USA). DFK167 was purchased from Enzyme Systems Products (Livermore, CA, USA). DAPT and L-685,458 were obtained from Calbiochem (San Diego, CA, USA). Cycloheximide, staurosporine, A23187, rapamycin, and etoposide were from Sigma.

Cell culture, cDNA transfection, RNAi, and mutant PS1-knockin mouse

HEK293 cells and MEFs derived from PS1- and/or PS2-knockout mice (63) were cultured in Dulbecco's modified Eagle medium containing 10% fetal bovine serum and 1% streptomycin/penicillin. Transfection of cDNA into HEK293 cells was carried out using Lipofectamine PLUS reagent (Invitrogen). RNAi using a duplex siRNA against FKBP38 was described (33). Retroviral infection of MEFs was performed as previously reported (64). Briefly, PLATE-E packaging cells were transfected with the pMXs vector carrying the cDNA encoding FKBP38, PS2, or PS2 CTF^{CAS} using FuGene-6 (Roche Diagnostics). Culture media were collected two days after transfection for use as viral stocks. Viral transfection was carried out by incubating MEFs with viral stock containing 10 μg/ml Polybrene. One day after infection, the medium was replaced with fresh medium containing 10% fetal bovine serum. Infection efficiency was more than 95% in this study, as estimated from a control experiment using pMXs-β-galactosidase.

Generation and characterization of FAD-linked I213T-PS1-knockin mice was described previously (44). Brains were removed from two mice for each genotype (WT and heterozygous and homozygous mutants) and were homogenized with a Polytron PT1300D homogenizer (Kinematica, Littau-Luzern, Switzerland). Nuclei and cell debris were removed by centrifugation at 1,500*g* for 10 min. The postnuclear supernatants were subjected to subcellular fractionation.

Immunoblotting and immunoprecipitation

Cells were lysed in lysis buffer (25 mM HEPES, pH 7.5, 150 mM NaCl, 2 mM EDTA, 10% glycerol, and a mixture of protease inhibitors) containing 1% 3-[(3-cholamidopropyl)dimethylammonio]-2-hydroxy-1-propanesulfonic acid (CHAPSO). Protein concentration was determined using the micro DC protein assay kit (BioRad, Hercules, CA, USA). Immunoblotting was performed as previously described (62). The same amount of proteins from cell lysates was loaded in each lane. For immunoprecipitation, lysates of cultured cells or murine brains were pre-cleared with protein A-Sepharose CL-4B (Amersham Biosciences, Uppsala, Sweden) and were then incubated overnight at 4ºC with the appropriate antibody and protein A-Sepharose. The immunoprecipitates were washed three times with lysis buffer and were analyzed by immunoblotting.

Glycerol velocity gradient centrifugation

Glycerol velocity gradient centrifugation was carried out as previously described (35). HEK293 cells were disrupted in a Dounce homogenizer, and nuclei and large cell debris were sedimented by centrifugation at 1,500*g* for 10 min. Vesicle pellets were prepared from the postnuclear supernatants by centrifugation at 100,000*g* for 1 h and then lysed in buffer containing 1% CHAPSO. The lysates were layered onto a 15% to 30% (w/v) linear continuous glycerol gradient and centrifuged at 36,000*g* for 18 h. Fractions were collected from the bottom to give 20 fractions of 600 μl. The first eight fractions from the bottom were discarded, and the remaining fractions were analyzed by immunoblotting. Ferritin (440 kDa), β amylase (200 kDa), lactate dehydrogenase (140 kDa) and bovine serum albumin (67 kDa) are used as molecular weight markers.

Assessment of cell viability, apoptosis, and cytochrome c translocation

MEFs were treated with vehicle (DMSO), 2 μM staurosporine, or 10 μg/ml A23187 for 24 h in culture plates. Cell viability was evaluated by an MTT conversion assay. At the end of treatment period, 10 μl of MTT solution (5 mg/ml) was added to 100 μl of culture medium in each well of a 96-well plate. After 4 h incubation, 100 μl of MTT solubilization solution (isopropanol with 0.04 N HCl) was added to each well and mixed. The absorbance (570 nm) in each well was measured with a plate reader. Apoptosis was quantified with an apoptosis detection kit (MBL, Nagoya, Japan). After staining with annexin V-fluorescein isothiocyanate (FITC) and PI, apoptotic cells showed green fluorescence, and dead cells showed both red and green fluorescence as visualized by fluorescence

microscopy. Both bright-field and fluorescence images were obtained from arbitrary selected areas for each well in the 24-well plate using an IX71 microscope (Olympus, Tokyo, Japan). The percentage of annexin V-FITC- and/or PI-positive cells was determined by direct cell counting. For each value, approximately 1000 cells were counted from 10 images. For the cytochrome *c* translocation assay, cells were harvested in a hypotonic buffer (20 mM HEPES, pH 7.4, 10 mM $MgCl_2$, 42 mM KCl, and a mixture of protease inhibitors) and passed once through a 30-gauge needle. After sedimenting the crude nuclear fraction, the postnuclear supernatant was further centrifuged at 15,000*g* for 30 min to yield a crude membrane fraction. The supernatant was used as a cytosolic fraction. Both fractions were then subjected to immunoblotting with an anti-cytochrome *c* antibody.

Semi-quantitative RT-PCR and pulse-chase experiment

For semi-quantitative RT-PCR, total cellular RNA was isolated from MEFs using TRIzol reagent (Invitrogen). OneStep RT-PCR amplification (Qiagen, Valencia, CA, USA) was carried out with 100 ng total RNA and primer pairs specific for FKBP38, Bcl-2 or β-actin. Products were separated by electrophoresis on a 1.2% agarose gel, which was then stained with ethidium bromide. To identify the exponential amplification phase, 15, 20, 25, 30, and 35 PCR cycles were tested.

For pulse-chase experiment, MEFs were incubated for 1 h in Met- and Cys-free DMEM (Invitrogen) and were then labeled for 1 h with 50 μCi/ml [^{35}S] Met and [^{35}S] Cys (ICN Biomedicals, Irvine, CA, USA). Media were then replaced with complete medium for indicated times, after which cells were lysed in lysis buffer. Lysates were subjected to immunoprecipitation with anti-FKBP38 or anti-Bcl-2 antibody, and the immunoprecipitates were separated by SDS-PAGE. Gels were dried and analyzed with an electronic autoradiography imager (Packard Instruments, Meriden, CT, USA).

Assessment of subcellular localization of FKBP38 and Bcl-2

For immunocytochemistry, cells were fixed with 4% paraformaldehyde for 15 min and then permeabilized with 0.1% Triton X-100 for 5 min. Nonspecific antibody binding was blocked by incubating cells with 5% normal goat serum for 1 h. Fixed cells were incubated overnight at 4°C with a primary antibody, followed by reaction for 2 h with Alexa488-conjugated secondary antibody (Molecular Probes). Mitochondria were stained with MitoTracker Red (Molecular Probes) according to the manufacturer's instructions. Finally, the slides were analyzed with a LSM510 confocal

laser-scanning microscope (Zeiss, Oberkochen, Germany).

Subcellular fractionation by iodixanol gradient centrifugation was performed according to a previously described method with some modifications (65). The same amount of protein from resuspended vesicle preparations was applied to the top of a 2.5% to 30% (v/v) linear iodixanol gradient (Axis-Shield, Oslo, Norway) and was separated by centrifugation for 3 h at 200,000*g*. Sequential 1-ml fractions were then collected from the bottom of the centrifuge tube and were analyzed by immunoblotting.

ACKNOWLEDGEMENTS

We are grateful to Dr. Bart De Strooper for the mouse embryonic fibroblasts, Dr. Toshio Kitamura for a retrovirus vector and PLATE-E cells, and Miwako Nishikawa for technical assistance. We also acknowledge the Central Laboratory of the Shiga University of Medical Science for assistance in DNA sequencing and immunocytochemical studies by confocal laser microscopy. This work was supported in part by a Grant-in-Aid for Scientific Research from MEXT, Japan to M. N. and by grants from the Life Science Foundation and the Uehara Memorial Foundation to M. N.

References

1. Newmeyer, D.D, and Ferguson-Miller, S. (2003) Mitochondria: releasing power for life and unleashing the machineries of death. *Cell* **112**, 481-490.

2. Tsujimoto, Y. (2003) Cell death regulation by the Bcl-2 protein family in the mitochondria. *J. Cell Physiol.* **195**, 158-167.

3. Green, D.R., and Kroemer, G. (2004) The pathophysiology of mitochondrial cell death. *Science* **305**, 626-629.

4. Germain, M. and Shore, G.C. (2003) Cellular distribution of Bcl-2 family proteins. *Sci. STKE* **2003**, pe10.

5. Yuan, J. and Yankner, B.A. (2000) Apoptosis in the nervous system. *Nature* **407**, 802-809.

6. Yankner, B.A. (1996) Mechanisms of neuronal degeneration in Alzheimer's disease. *Neuron* **16**, 921-932.

7. Dickson, D.W. (2004) Apoptotic mechanisms in Alzheimer neurofibrillary degeneration: cause or effect? *J. Clin. Invest.* **114**, 23-27.

8. Jellinger, K.A. (2001) Cell death mechanisms in neurodegeneration. *J. Cell Mol. Med.* **5**, 1-17.

9. Cribbs, D.H., Poon, W.W., Rissman, R.A. and Blurton-Jones, M. (2004) Caspase-mediated degeneration in Alzheimer's disease. *Am. J. Pathol.* **165**, 353-355.

10. St George-Hyslop, P.H. (2000) Molecular genetics of Alzheimer's disease. *Biol. Psychiatry* **47**, 183-199.

11. Thinakaran, G., Harris, C.L., Ratovitski, T., Davenport, F., Slunt, H.H., Price, D.L., Borchelt, D.R. and Sisodia, S.S. (1997) Evidence that levels of presenilins (PS1 and PS2) are coordinately regulated by competition for limiting cellular factors. *J. Biol. Chem.* **272**, 28415-28422.

12. Vito, P., Lacana, E. and D'Adamio, L. (1996) Interfering with apoptosis: Ca(2+)-binding protein ALG-2 and Alzheimer's disease gene ALG-3. *Science* **271**, 521-525.

13. Wolozin, B., Iwasaki, K., Vito, P., Ganjei, J.K., Lacana, E., Sunderland, T., Zhao, B., Kusiak, J.W., Wasco, W. and D'Adamio, L. (1996) Participation of presenilin 2 in apoptosis: enhanced basal activity conferred by an Alzheimer mutation. *Science* **274**, 1710-1713.

14. Vito, P., Wolozin, B., Ganjei, J.K., Iwasaki, K., Lacana, E. and D'Adamio, L. (1996) Requirement

of the familial Alzheimer's disease gene PS2 for apoptosis. Opposing effect of ALG-3. *J. Biol. Chem.* **271**, 31025-31028.

15. Deng, G., Pike, C.J. and Cotman, C.W. (1996) Alzheimer-associated presenilin-2 confers increased sensitivity to apoptosis in PC12 cells. *FEBS lett.* **397**, 50-54.
16. Janicki, S. and Monteiro, M.J. (1997) Increased apoptosis arising from increased expression of the Alzheimer's disease-associated presenilin-2 mutation (N141I). *J. Cell Biol.* **139**, 485-495.
17. Guo, Q., Sopher, B.L., Furukawa, K., Pham, D.G., Robinson, N., Martin, G.M. and Mattson, M.P. (1997) Alzheimer's presenilin mutation sensitizes neural cells to apoptosis induced by trophic factor withdrawal and amyloid β-peptide: involvement of calcium and oxyradicals. *J. Neurosci.* **17**, 4212-4222.
18. Wolozin, B., Alexander, P. and Palacino, J. (1998) Regulation of apoptosis by presenilin 1. *Neurobiol. Aging* **19**, S23-27.
19. Kovacs, D.M., Mancini, R., Henderson, J., Na, S.J., Schmidt, S.D., Kim, T.W., and Tanzi, R.E. (1999) Staurosporine-induced activation of caspase-3 is potentiated by presenilin 1 familial Alzheimer's disease mutations in human neuroglioma cells. *J. Neurochem.* **73**, 2278-2285.
20. Guo, Q., Sebastian, L., Sopher, B.L., Miller, M.W., Ware, C.B., Martin, G.M. and Mattson, M.P. (1999) Increased vulnerability of hippocampal neurons from presenilin-1 mutant knock-in mice to amyloid β-peptide toxicity: central roles of superoxide production and caspase activation. *J. Neurochem.* **72**, 1019-1029.
21. Tanii, H., Ankarcrona, M., Flood, F., Nilsberth, C., Mehta, N.D., Perez-Tur, J., Winblad, B., Benedikz, E. and Cowburn, R.F. (2000) Alzheimer's disease presenilin-1 exon 9 deletion and L250S mutations sensitize SH-SY5Y neuroblastoma cells to hyperosmotic stress-induced apoptosis. *Neuroscience* **95**, 593-601.
22. Terro, F., Czech, C., Esclaire, F., Elyaman, W., Yardin, C., Baclet, M.C., Touchet, N., Tremp, G., Pradier, L. and Hugon, J. (2000) Neurons overexpressing mutant presenilin-1 are more sensitive to apoptosis induced by endoplasmic reticulum-Golgi stress. *J. Neurosci. Res.* **69**, 530-539.
23. Alves da Costa, C., Paitel, E., Mattson, M.P., Amson, R., Telerman, A., Ancolio, K. and Checler, F. (2002) Wild-type and mutated presenilins 2 trigger p53-dependent apoptosis and down-regulate

presenilin 1 expression in HEK293 human cells and in murine neurons. *Proc. Natl. Acad. Sci. USA.* **99**, 4043-4048.

24. Kim, T.W., Pettingell, W.H., Jung, Y.K., Kovacs, D.M. and Tanzi, R.E. (1997) Alternative cleavage of Alzheimer-associated presenilins during apoptosis by a caspase-3 family protease. *Science* **277**, 373-376.

25. Vito, P., Ghayur, T. and D'Adamio, L. (1997) Generation of anti-apoptotic presenilin-2 polypeptides by alternative transcription, proteolysis, and caspase-3 cleavage. *J. Biol. Chem.* **272**, 28315-28320.

26. Vezina. J., Tschopp, C., Andersen, E. and Muller, K. (1999) Overexpression of a C-terminal fragment of presenilin 1 delays anti-Fas induced apoptosis in Jurkat cells. *Neurosci. Lett.* **263**, 65-68.

27. De Strooper, B. (2003) Aph-1, Pen-2, and Nicastrin with Presenilin generate an active γ-Secretase complex. *Neuron* **38**, 9-12.

28. Kang, D.E., Soriano, S., Xia, X., Eberhart, C.G., De Strooper, B., Zheng, H. and Koo, E.H. (2002) Presenilin couples the paired phosphorylation of β-catenin independent of axin: implications for β-catenin activation in tumorigenesis. *Cell* **110**, 751-762.

29. Yoo, A.S., Cheng, I., Chung, S., Grenfell, T.Z., Lee, H., Pack-Chung, E., Handler, M., Shen, J., Xia, W., Tesco, G. *et al.* (2000) Presenilin-mediated modulation of capacitative calcium entry. *Neuron* **27**, 561-572.

30. Lam, E., Martin, M. and Wiederrecht, G. (1995) Isolation of a cDNA encoding a novel human FK506-binding protein homolog containing leucine zipper and tetratricopeptide repeat motifs. *Gene* **160**, 297-302.

31. Pedersen, K.M., Finsen, B., Celis, J.E. and Jensen, N.A. (1999) muFKBP38: a novel murine immunophilin homolog differentially expressed in Schwannoma cells and central nervous system neurons in vivo. *Electrophoresis* **20**, 249-255.

32. Adrain, C., Creagh, E.M. and Martin, S.J. (2003) Defying death: showing Bcl-2 the way home. *Nat. Cell Biol.* **5**, 9-11.

33. Shirane, M. and Nakayama, K.I. (2003) Inherent calcineurin inhibitor FKBP38 targets Bcl-2 to

mitochondria and inhibits apoptosis. PEN-2 is an integral component of the γ-secretase complex required for coordinated expression of presenilin and nicastrin. *Nat. Cell Biol.* **5**, 28-37.

34. Alberici, A., Moratto, D., Benussi, L., Gasparini, L., Ghidoni, R., Gatta, L.B., Finazzi, D., Frisoni, G.B., Trabucchi, M., Growdon, J.H. *et al.* (1999) Presenilin 1 protein directly interacts with Bcl-2. *J. Biol. Chem.* **274**, 30764-30769.

35. Yu, G., Chen, F., Levesque, G., Nishimura, M., Zhang, D.M., Levesque, L., Rogaeva, E., Xu, D., Liang, Y., Duthie, M. *et al.* (1998) The presenilin 1 protein is a component of a high molecular weight intracellular complex that contains β-catenin. *J. Biol. Chem.* **273**, 16470-16475.

36. Harrison, T. and Beher, D. (2003) γ-Secretase inhibitors--from molecular probes to new therapeutics? *Prog. Med. Chem.* **41**, 99-127.

37. Krajewski, S., Tanaka, S., Takayama, S., Schibler, M.J., Fenton, W. and Reed, J.C. (1993) Investigation of the subcellular distribution of the bcl-2 oncoprotein: residence in the nuclear envelope, endoplasmic reticulum, and outer mitochondrial membranes. *Cancer Res.* **53**, 4701-4714.

38. Kovacs, D.M., Fausett, H.J., Page, K.J., Kim, T.W., Moir, R.D., Merriam, D.E., Hollister, R.D., Hallmark, O.G., Mancini, R., Felsenstein, K.M. *et al.* (1996) Alzheimer-associated presenilins 1 and 2: neuronal expression in brain and localization to intracellular membranes in mammalian cells. *Nat. Med.* **2**, 224-229.

39. Li, J., Xu, M., Zhou, H., Ma, J. and Potter, H. (1997) Alzheimer presenilins in the nuclear membrane, interphase kinetochores, and centrosomes suggest a role in chromosome segregation. *Cell* **90**, 917-927.

40. Ankarcrona, M. and Hultenby, K. (2002) Presenilin-1 is located in rat mitochondria. *Biochem. Biophys. Res. Commun.* **295**, 766-770.

41. Pratt, W.B. and Toft, D.O. (2003) Regulation of signaling protein function and trafficking by the hsp90/hsp70-based chaperone machinery. *Exp. Biol. Med.* **228**, 111-133.

42. Araki, W., Yuasa, K., Takeda, S., Takeda, K., Shirotani, K., Takahashi, K. and Tabira, T. (2001) Pro-apoptotic effect of presenilin 2 (PS2) overexpression is associated with down-regulation of Bcl-2 in cultured neurons. *J. Neurochem.* **79**, 1161-1168.

43. Mori, M., Nakagami, H., Morishita, R., Mitsuda, N., Yamamoto, K., Yoshimura, S., Ohkubo, N.,

Sato, N., Ogihara, T. and Kaneda, Y. (2002) N141I mutant presenilin-2 gene enhances neuronal cell death and decreases bcl-2 expression. *Life Sci*. **70**, 2567-2580.

44. Nakano, Y., Kondoh, G., Kudo, T., Imaizumi, K., Kato, M., Miyazaki, J.I., Tohyama, M., Takeda, J. and Takeda, M. (1999) Accumulation of murine amyloid β 42 in a gene-dosage-dependent manner in PS1 'knock-in' mice. *Eur. J. Neurosci*. **11**, 2577-25781.

45. Xie, J., Chang, X., Zhang, X., and Guo Q. (2001) Aberrant induction of Par-4 is involved in apoptosis of hippocampal neurons in presenilin-1 M146V mutant knock-in mice. *Brain Res*. **915**, 1-10.

46. Kaufmann, T., Schlipf, S., Sanz, J., Neubert, K., Stein, R. and Borner, C. (2003) Characterization of the signal that directs Bcl-X_L, but not Bcl-2, to the mitochondrial outer membrane. *J. Cell Biol*. **160**, 53-64.

47. Tagami, S., Eguchi, Y., Kinoshita, M., Takeda, M. and Tsujimoto, Y. (2000) A novel protein, RTN-X_S, interacts with both Bcl-X_L and Bcl-2 on endoplasmic reticulum and reduces their anti-apoptotic activity. *Oncogene* **19**, 5736-5746.

48. Passer, B.J., Pellegrini, L., Vito, P., Ganjei, J.K. and D'Adamio, L. (1999) Interaction of Alzheimer's presenilin-1 and presenilin-2 with Bcl-X(L). A potential role in modulating the threshold of cell death. *J. Biol. Chem*. **274**, 24007-24013.

49. Alves da Costa, C., Mattson, M.P., Ancolio, K., and Checler, F. (2003) The C-terminal fragment of presenilin 2 triggers p53-mediated staurosporine-induced apoptosis, a function independent of the presenilinase-derived N-terminal counterpart. *J. Biol. Chem*. **278**, 12064-12069.

50. Sun, J., Li, M., Han, J., and Gu, J. (2001) Sensitization of differentiated PC12 cells to apoptosis by presenilin-2 is mediated by p38. *Biochem. Biophys. Res. Commun*. **287**, 536-541.

51. Weihl, C.C., Ghadge, G.D., Kennedy, S.G., Hay, N., Miller, R.J., and Roos, R.P. (1999) Mutant presenilin-1 induces apoptosis and downregulates Akt/PKB. *J. Neurosci*. **19**, 5360-5369.

52. Katayama, T., Imaizumi, K., Sato, N., Miyoshi, K., Kudo, T., Hitomi, J., Morihara, T., Yoneda, T., Gomi, F., Mori, Y. *et al*. (1999) Presenilin-1 mutations downregulate the signalling pathway of the unfolded-protein response. *Nat. Cell Biol*. **1**, 479-485.

53. Zhang, Z., Hartmann, H., Do, V.M., Abramowski, D., Sturchler-Pierrat, C., Staufenbiel, M.,

Sommer, B., van de Wetering, M., Clevers, H., Saftig, P. *et al*. (1998) Destabilization of β-catenin by mutations in presenilin-1 potentiates neuronal apoptosis. *Nature* **395**, 698-702.

54. Mattson, M.P., Zhu, H., Yu, J., and Kindy, M.S. (2000) Presenilin-1 mutation increases neuronal vulnerability to focal ischemia in vivo and to hypoxia and glucose deprivation in cell culture: involvement of perturbed calcium homeostasis. *J. Neurosci*. **20**, 1358-1364.

55. Steiner, H., Capell, A., Pesold, B., Citron, M., Kloetzel, P.M., Selkoe, D.J., Romig, H., Mendla, K. and Haass, C. (1998) Expression of Alzheimer's disease-associated presenilin-1 is controlled by proteolytic degradation and complex formation. *J. Biol. Chem*. **273**, 32322-32331.

56. Annaert, W.G., Esselens, C., Baert, V., Boeve, C., Snellings, G., Cupers, P., Craessaerts, K. and De Strooper, B. (2001) Interaction with telencephalin and the amyloid precursor protein predicts a ring structure for presenilins. *Neuron* **32**, 579-589.

57. Esselens, C., Oorschot, V., Baert, V., Raemaekers, T., Spittaels, K., Serneels, L., Zheng, H., Saftig, P., De Strooper, B., Klumperman, J. *et al*. (2004) Presenilin 1 mediates the turnover of telencephalin in hippocampal neurons via an autophagic degradative pathway. *J. Cell Biol*. 166, 1041-1054.

58. Selkoe, D.J. (2002) Deciphering the genesis and fate of amyloid β-protein yields novel therapies for Alzheimer disease. *J. Clin. Invest*. **110**, 1375-1381.

59. Walsh, D.M., Klyubin, I., Fadeeva, J.V., Cullen, W.K., Anwyl, R., Wolfe, M.S., Rowan, M.J. and Selkoe, D.J. (2002) Naturally secreted oligomers of amyloid β protein potently inhibit hippocampal long-term potentiation in vivo. *Nature* **416**, 535-539.

60. Lambert, M.P., Barlow, A.K., Chromy, B.A., Edwards, C., Freed, R., Liosatos, M., Morgan, T.E., Rozovsky, I., Trommer, B., Viola, K.L. *et al*. (1998) Diffusible, nonfibrillar ligands derived from Aβ1-42 are potent central nervous system neurotoxins. *Proc. Natl. Acad. Sci. USA* **95**, 6448-6453.

61. Eckert, A., Keil, U., Marques, C.A., Bonert, A., Frey, C., Schussel, K. and Muller, W.E. (2003) Mitochondrial dysfunction, apoptotic cell death, and Alzheimer's disease. *Biochem. Pharmacol*. **66**, 1627-1634.

62. Nishimura, M., Yu, G., Levesque, G., Zhang, D.M., Ruel, L., Chen, F., Milman, P., Holmes, E., Liang, Y., Kawarai, T. *et al*. (1999) Presenilin mutations associated with Alzheimer disease cause

defective intracellular trafficking of β-catenin, a component of the presenilin protein complex. *Nat. Med.* **5**, 164-169.

63. Herreman, A., Serneels, L., Annaert, W., Collen, D., Schoonjans, L. and De Strooper, B. (2000) Total inactivation of γ-secretase activity in presenilin-deficient embryonic stem cells. *Nat. Cell Biol.* **2**, 461-462.

64. Onishi, M., Kinoshita, S., Morikawa, Y., Shibuya, A., Phillips, J., Lanier, L.L., Gorman, D.M., Nolan, G.P, Miyajima, A. and Kitamura, T. (1996) Applications of retrovirus-mediated expression cloning. *Exp. Hematol.* **24**, 324-329.

65. Gu, Y., Chen, F., Sanjo, N., Kawarai, T., Hasegawa, H., Duthie, M., Li, W., Ruan, X., Luthra, A., Mount, H.T. *et al.* (2003) APH-1 interacts with mature and immature forms of presenilins and nicastrin and may play a role in maturation of presenilin-nicastrin complexes. *J. Biol. Chem.* **278**, 7374-7380.

Figure legends

Figure 1

PS1/2 specifically interact with FKBP38. **(A)** Coimmunoprecipitation of transfected PS1/2 and FKBP38. HEK293 cells were transiently cotransfected with PS1 (left panels) or PS2 (right panels) together with FKBP38-Myc, CyP40-Myc, FKBP51-Myc, or FKBP52-Myc. Cell lysates (Input) and immunoprecipitates obtained with an anti-Myc antibody (IP) were analyzed by immunoblotting. **(B)** Coimmunoprecipitation of endogenous PS1/2 and FKBP38. Protein extracts from mouse brains were subjected to immunoprecipitation with preimmune serum or an antibody against PS1 CTF, PS2 CTF, Bcl-2, calnexin, or FKBP38. Total extract (Input) and immunoprecipitates were immunoblotted with an anti-FKBP38 antibody. **(C)** Coimmunoprecipitation of PS1/2 and FKBP38$^{\Delta TM}$. Lysates from HEK293 cells transiently transfected with FKBP38-HA and FKBP38$^{\Delta TM}$-HA were subjected to immunoprecipitation with an anti-PS1 CTF or anti-PS2 CTF antibody. Cell lysates (Input) and immunoprecipitates were immunoblotted with an anti-HA antibody. (**D**) Coimmunoprecipitation in lysates from PS1/2- and/or FKBP38-depleted cells. Cell lysates were prepared from native, PS1/2-null, FKBP38-knockdown (k/d), or PS1/2-null/FKBP38-k/d MEFs. Total cell lysates (Input) and immunoprecipitates with preimmune serum (P) or anti-Bcl-2 antibody (B) were immunoblotted with an antibody against PS1 CTF, PS2 CTF, FKBP38, or Bcl-2.

Figure 2

FKBP38 and Bcl-2 are incorporated into macromolecular complexes of PS1/2. **(A)** Glycerol velocity gradient centrifugation followed by immunoblotting for PS1, PS2, FKBP38, and Bcl-2. Extracts from native HEK293 cells were used for analysis of PS1, FKBP38, or Bcl-2, and PS2-transfected HEK293 cells were used for PS2 analysis. The positions of molecular weight markers are indicated at the top of the panel. Results are representative of three independent experiments. **(B)** Coimmunoprecipitation with anti-PS2 CTF antibody from fractionated samples in **A**. Immunoprecipitates were subjected to immunoblotting with an antibody against FKBP38, Bcl-2, or PS2 CTF.

Figure 3

PS1 and PS2 sensitize MEFs to apoptosis. Native, PS1-null, PS2-null, and PS1/2-null MEFs were treated for 24 h with vehicle (DMSO), 2 μM staurosporine (STS), or 10 μg/ml A23187. **(A)** The relative viability was estimated by an MTT assay. Data represent the means ± SD (n = 24). *$p < 0.001$ by one-way ANOVA with Dunnett's *post-hoc* test. **(B)** The percentage of annexin V- and/or PI-positive apoptotic MEFs. Data represent the means ± SD (n = 3). *$p < 0.001$ by one-way ANOVA with Dunnett's *post-hoc* test. **(C)** Cytochrome *c* translocation assay. Cytosol (C) and membrane (M) fractions from the treated MEFs were analyzed by immunoblotting with an anti-cytochrome *c* antibody. Results are representative of three independent experiments.

Figure 4

PS1/2 promote the degradation of FKBP38 and Bcl-2. **(A)** Immunoblotting of native and PS1/2-null MEF lysates for endogenous FKBP38, Bcl-2, and β-actin. Equal amounts of protein (20 μg) were loaded in each lane. **(B)** Semi-quantitative RT-PCR analysis of FKBP38 or Bcl-2 mRNA in native and PS1/2-null MEFs. PCR products amplified after 20 and 30 cycles are shown. RT-PCR for β-actin served as an internal standard. **(C)** Immunoblot analysis showing degradation of FKBP38 and Bcl-2 proteins in native and PS1/2-null MEFs after treatment with the protein synthesis inhibitor cycloheximide (50 μg/ml). Equal amounts of protein (20 μg) were loaded in each lane. The intensity of the bands was determined by densitometry. The graphs show the average relative intensity from three independent blots. Error bars represent the SD. **(D)** Pulse-chase experiment for FKBP38 in native and PS1/2-null MEFs. Bands at a chase time = 0 represent the rates of translation.

Figure 5

FKBP38 is not a substrate for γ-secretase. **(A)** Culture media, cytosol fractions, and membrane fractions from native and PS1/2-null MEFs were immunoblotted with an anti-FKBP38 antibody. **(B)** HEK293 cells were treated with vehicle (DMSO) or the γ-secretase inhibitors DFK167 (100 μM), DAPT (2 μM), or L-685,458 (1 μM) for 24 h. Cell lysates were immunoblotted with an anti-FKBP38 or anti-APP antibody. **(C)** HEK293 cells transiently transfected with FKBP38 fused to GFP

(FKBP38-GFP) were cultured in the absence or presence of DFK167 (100 μM) for 24 h. Cell lysates were immunoblotted with an anti-GFP antibody.

Figure 6

PS1/2 regulate the subcellular distribution of FKBP38 and Bcl-2. **(A)** Double fluorescence labeling confocal microscopy showing the localization of FKBP38 (green) and mitochondria (MitoTracker; red) in native and PS1/2-null MEFs. Merged images show mitochondrial localization of FKBP38 as yellow fluorescence. **(B)** Double-staining confocal images showing the localization of Bcl-2 (green) and mitochondria (MitoTracker; red). Mitochondrial Bcl-2 is shown in yellow fluorescence. **(C)** Subcellular fractionation by iodixanol gradient centrifugation of native and PS1/2-null MEFs. Fractionated samples (indicated at the bottom) were analyzed by immunoblotting with an antibody against PS1 CTF, FKBP38, or Bcl-2. The distribution patterns of the mitochondrial marker cyclooxygenase-IV (COX-IV), the ER marker calnexin, and the trans-Golgi network marker adaptin-γ are shown in the upper panels. **(D)** Iodixanol fractionation of FKBP38 knockdown (k/d) MEFs. Native and PS1/2-null MEFs were treated with a duplex siRNA against FKBP38 (FKBP38-k/d in native, and FKBP38-k/d in PS1/2-null, respectively), and the cell homogenates were subjected to iodixanol fractionation. Fractionated samples were immunoblotted with an anti-Bcl-2 antibody. Results are representative of three independent experiments.

Figure 7

Pro-apoptotic activity of PS1/2 correlates with a reduction in mitochondrial Bcl-2. **(A)** MTT assay of MEFs expressing various constructs of PS2 and/or FKBP38. WT PS2, WT PS2 + FKBP38, FAD-linked (N141I and M239V) PS2, or loss-of-function mutant (D366A) PS2 was transfected by a retrovirus into PS1/2-null MEFs. PS2 CTF^{CAS} was transfected into native MEFs. Then, MEFs were treated for 24 h with vehicle (DMSO) or staurosporine (2 μM). Relative viability is shown. Results represent the means ± SD (n = 24). *$p < 0.001$ by one-way ANOVA with Dunnett's *post-hoc* test. **(B)** Immunoblotting of total cell lysates from PS1/2-null, native, and PS2-overexpressing (OE) MEFs. Blots were probed with an antibody against PS2 CTF, PS1 CTF, FKBP38, Bcl-2, or β-actin. Equal

amounts of protein (20 μg) were loaded in each lane. **(C)** Subcellular fractionation by iodixanol gradient centrifugation of native MEFs and MEFs overexpressing WT PS2, WT PS2 + FKBP38, N141I-PS2, PS2 CTF^{CAS}, or D366A-PS2. Fractionated samples were immunoblotted with anti-Bcl-2 antibody. The distribution of organelle markers is shown in Figure 6C. The relative intensity of the bands for Bcl-2 in tentative mitochondrial fractions (lanes 1-5) and in whole lanes was determined by densitometry. The graph shows the average ratios of mitochondrial to total Bcl-2 from three independent blots. Error bars represent the SD. $*p < 0.05$ by one-way ANOVA with Dunnett's *post-hoc* test. **(D)** Iodixanol fractionation followed by immunoblotting shows the distribution of transfected PS2 in PS1/2-null MEFs. **(E)** Iodixanol fractionation of brains from FAD-linked I213T-PS1-knockin mice. Brain homogenates were prepared from WT, heterozygous (Mut PS1-k/i-hetero), and homozygous (Mut-PS1-k/i-homo) mice. Fractionated samples were immunoblotted with an antibody against FKBP38 (left panels) or Bcl-2 (right panels). Results are representative of three independent experiments.

The abbreviations used

PS, presenilin;

FKBP, FK506-binding protein;

AD, Alzheimer's disease;

FAD, familial Alzheimer's disease;

Aβ, amyloid β;

APP, amyloid β-precursor protein;

WT, wild-type;

TPR, tetratricopeptide repeat;

MEF, mouse embryonic fibroblast;

HEK293 cell, human embryonic kidney 293 cell;

ER, endoplasmic reticulum;

FL, full length;

NTF, N-terminal fragment;

CTF, C-terminal fragment;

CHAPSO, 3-[(3-cholamidopropyl)dimethylammonio]-2-hydroxy-1-propanesulfonic acid;

MTT, 3-(4,5-dimethylthiazal-2-yl)-2,5-diphenyltetrazolium bromide;

RNAi, RNA interference;

siRNA, small interfering RNA;

FITC, fluorescein isothiocyanate;

PI, propidium iodide;

HA, haemagglutinin A;

GFP, green fluorescent protein.

Figure 1

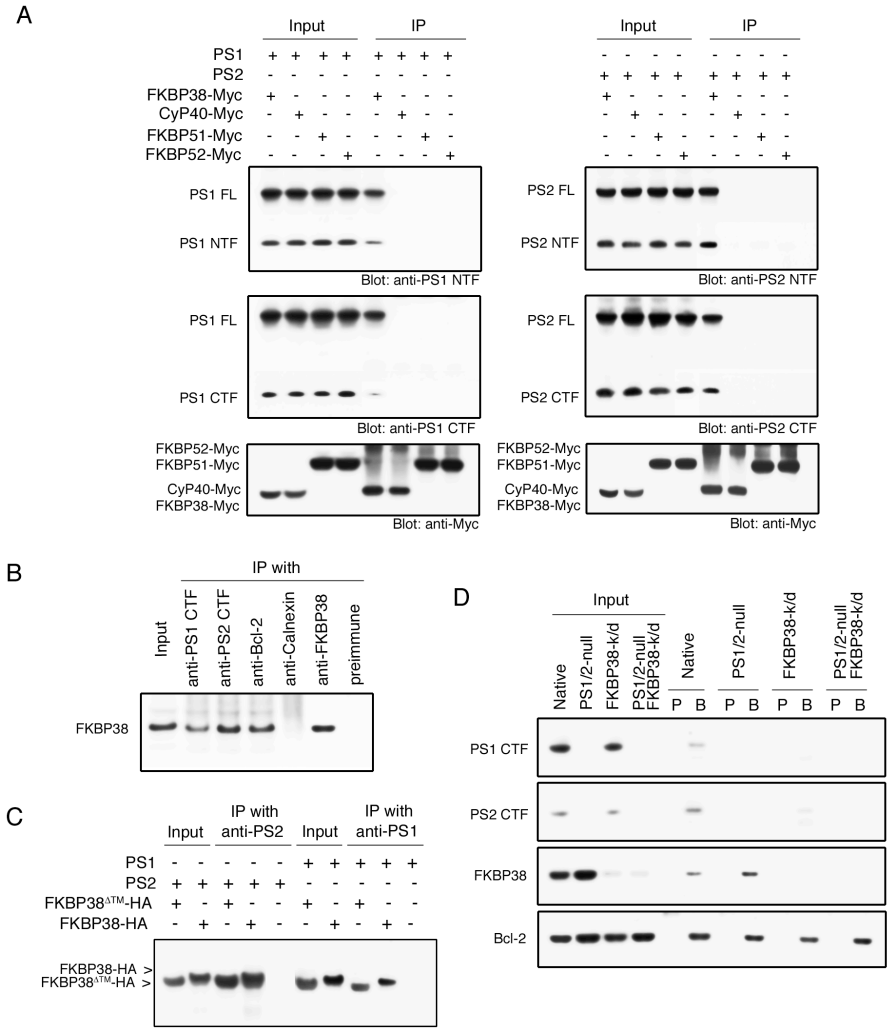
A
Input
IP
PS1
PS2
FKBP38-Myc
CyP40-Myc
FKBP51-Myc
FKBP52-Myc
PS1 FL
PS1 NTF
Blot: anti-PS1 NTF
PS2 FL
PS2 NTF
Blot: anti-PS2 NTF
PS1 CTF
Blot: anti-PS1 CTF
PS2 CTF
Blot: anti-PS2 CTF
Blot: anti-Myc
B
IP with
Input
anti-PS1 CTF
anti-PS2 CTF
anti-Bcl-2
anti-Calnexin
anti-FKBP38
preimmune
FKBP38
C
IP with anti-PS2
IP with anti-PS1
FKBP38-HA
FKBP38ΔTM-HA
D
Native
PS1/2-null
FKBP38-k/d
PS1/2-null FKBP38-k/d
P
B
Bcl-2

Figure 2

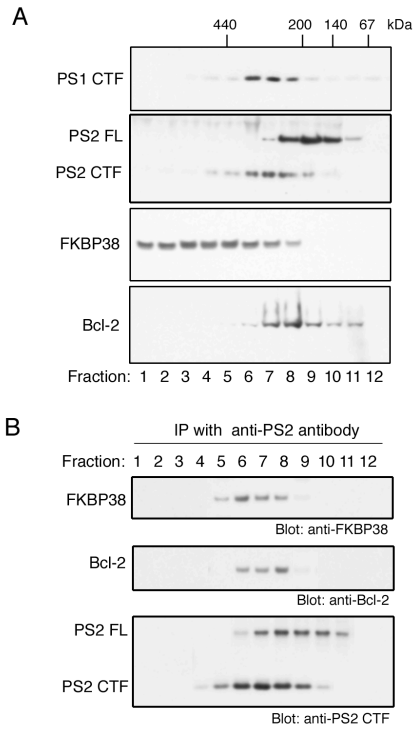
A
440
200
140
67
kDa
PS1 CTF
PS2 FL
PS2 CTF
FKBP38
Bcl-2
Fraction: 1 2 3 4 5 6 7 8 9 10 11 12
B
IP with anti-PS2 antibody
Fraction: 1 2 3 4 5 6 7 8 9 10 11 12
FKBP38
Blot: anti-FKBP38
Bcl-2
Blot: anti-Bcl-2
PS2 FL
PS2 CTF
Blot: anti-PS2 CTF

Figure 3

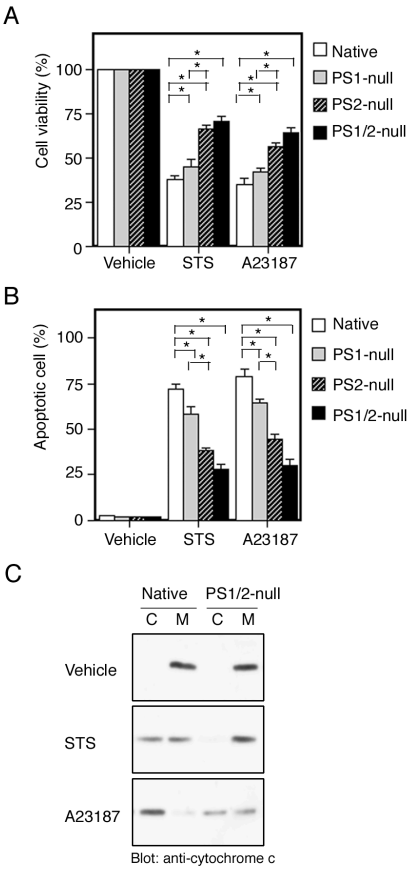
A
Cell viability (%)
100
75
50
25
0
Vehicle
STS
A23187
Native
PS1-null
PS2-null
PS1/2-null
B
Apoptotic cell (%)
100
75
50
25
0
Vehicle
STS
A23187
Native
PS1-null
PS2-null
PS1/2-null
C
Native
PS1/2-null
C
M
C
M
Vehicle
STS
A23187
Blot: anti-cytochrome c

Figure 4

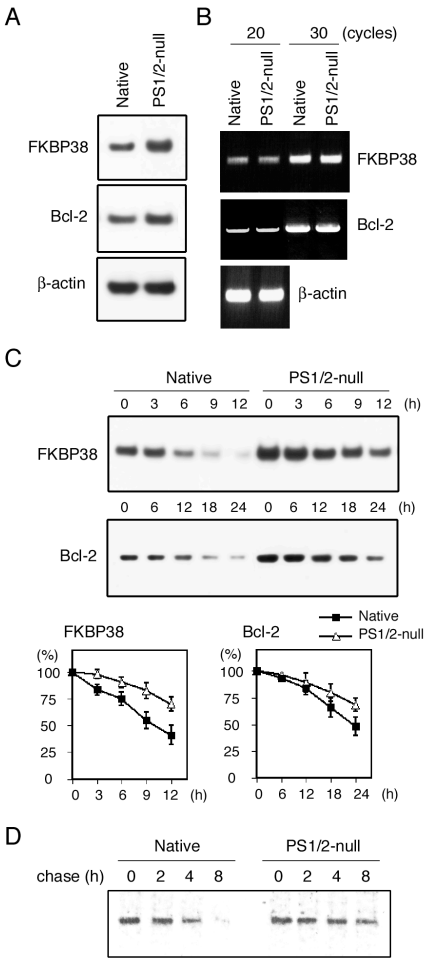
A
Native
PS1/2-null
FKBP38
Bcl-2
β-actin
B
20
30
(cycles)
Native
PS1/2-null
Native
PS1/2-null
FKBP38
Bcl-2
β-actin
C
Native
PS1/2-null
0 3 6 9 12 0 3 6 9 12 (h)
FKBP38
0 6 12 18 24 0 6 12 18 24 (h)
Bcl-2
FKBP38
Bcl-2
Native
PS1/2-null
(%)
100
75
50
25
0
0 3 6 9 12 (h)
0 6 12 18 24 (h)
D
Native
PS1/2-null
chase (h) 0 2 4 8 0 2 4 8

Figure 5

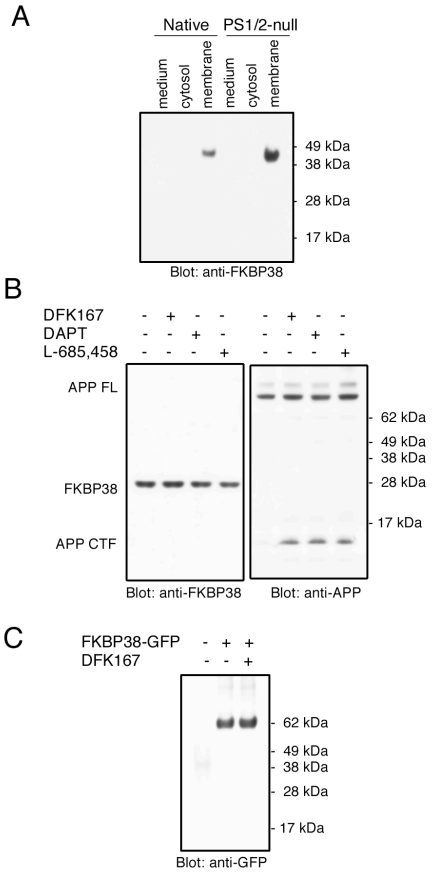
A
Native
PS1/2-null
medium
cytosol
membrane
medium
cytosol
membrane
49 kDa
38 kDa
28 kDa
17 kDa
Blot: anti-FKBP38
B
DFK167
DAPT
L-685,458
APP FL
FKBP38
APP CTF
62 kDa
49 kDa
38 kDa
28 kDa
17 kDa
Blot: anti-FKBP38
Blot: anti-APP
C
FKBP38-GFP
DFK167
62 kDa
49 kDa
38 kDa
28 kDa
17 kDa
Blot: anti-GFP

Figure 6

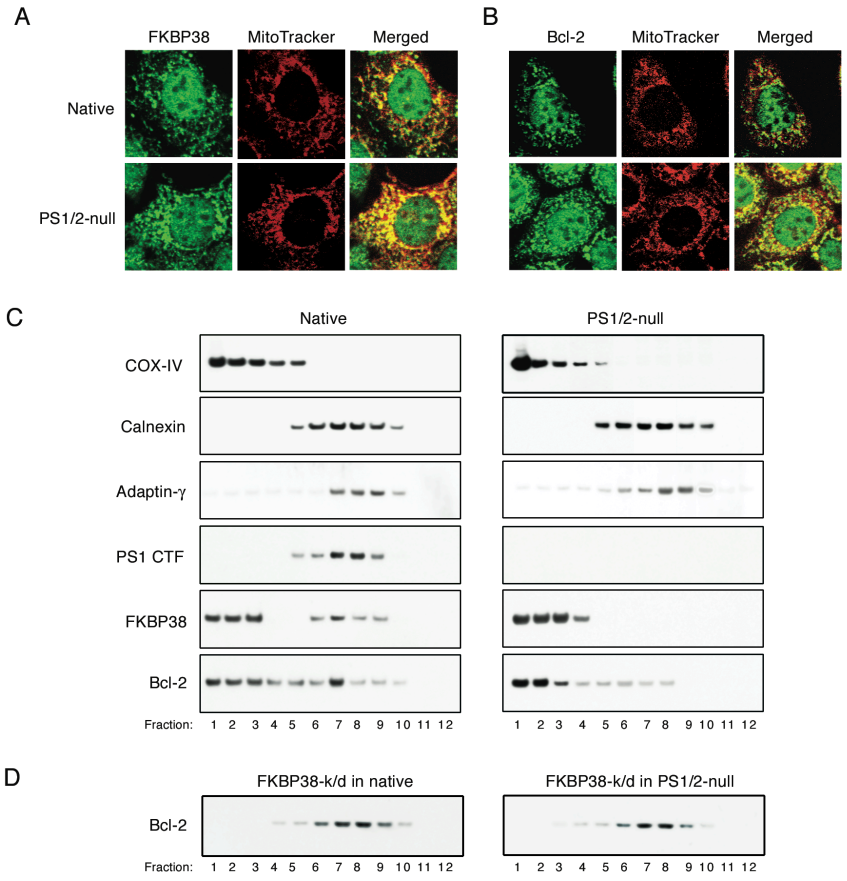
A
FKBP38
MitoTracker
Merged
Native
PS1/2-null
B
Bcl-2
MitoTracker
Merged
C
Native
PS1/2-null
COX-IV
Calnexin
Adaptin-γ
PS1 CTF
FKBP38
Bcl-2
Fraction: 1 2 3 4 5 6 7 8 9 10 11 12
D
FKBP38-k/d in native
FKBP38-k/d in PS1/2-null
Bcl-2
Fraction: 1 2 3 4 5 6 7 8 9 10 11 12

Figure 7

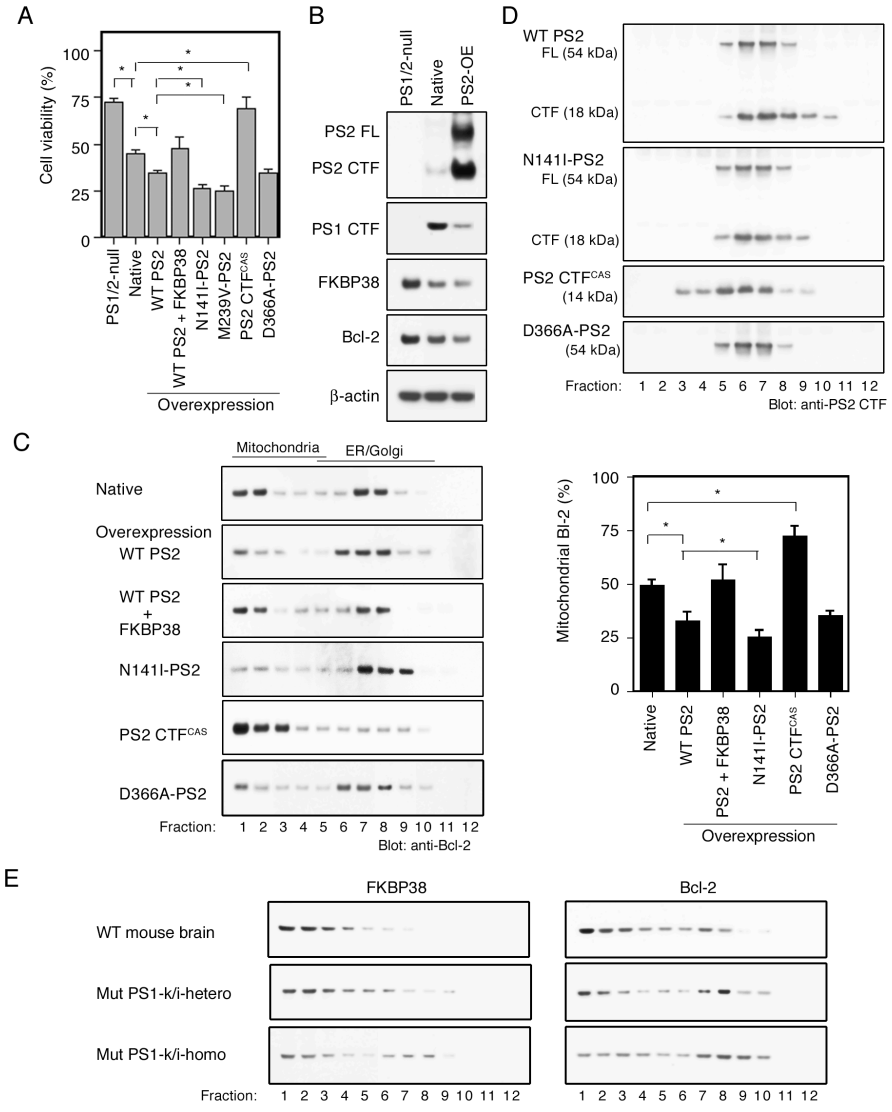
A
Cell viability (%)
100
75
50
25
0
PS1/2-null
Native
WT PS2
WT PS2 + FKBP38
N141I-PS2
M239V-PS2
PS2 CTFCAS
D366A-PS2
Overexpression
B
PS1/2-null
Native
PS2-OE
PS2 FL
PS2 CTF
PS1 CTF
FKBP38
Bcl-2
β-actin
D
WT PS2
FL (54 kDa)
CTF (18 kDa)
N141I-PS2
FL (54 kDa)
CTF (18 kDa)
PS2 CTFCAS
(14 kDa)
D366A-PS2
(54 kDa)
Fraction: 1 2 3 4 5 6 7 8 9 10 11 12
Blot: anti-PS2 CTF
C
Mitochondria
ER/Golgi
Native
Overexpression
WT PS2
WT PS2
+
FKBP38
N141I-PS2
PS2 CTFCAS
D366A-PS2
Fraction: 1 2 3 4 5 6 7 8 9 10 11 12
Blot: anti-Bcl-2
Mitochondrial Bl-2 (%)
100
75
50
25
0
Native
WT PS2
PS2 + FKBP38
N141I-PS2
PS2 CTFCAS
D366A-PS2
Overexpression
E
FKBP38
Bcl-2
WT mouse brain
Mut PS1-k/i-hetero
Mut PS1-k/i-homo
Fraction: 1 2 3 4 5 6 7 8 9 10 11 12
1 2 3 4 5 6 7 8 9 10 11 12